

# Dynamic behavior and mechanical features of wool felt

A. Stulov, Tallinn, Estonia

Received February 24, 2004  
Published online: May 5, 2004 © Springer-Verlag 2004

**Summary.** Experimental testing of piano hammers, which consist of a wood core covered with several layers of compressed wool felt demonstrates, that all hammers have the hysteretic type of the force-compression characteristics. It is shown, that different mathematical hysteretic models can describe the dynamic behavior of the hammer felt. In addition to the four-parameter nonlinear hysteretic felt model, another new three-parameter hysteretic model is presented. Both models are based on the assumption that the hammer felt made of wool is a microstructured material possessing history-dependent properties. The equivalence of these models is proved for all realistic values of hammer velocity.

## 1 Introduction

The felt made of wool is a miraculous material indeed. Almost two hundred years this material is used for piano hammer manufacturing. In spite of the endless attempts to match a more suitable material for the piano hammer, the felt is a unique coating matter of wooden mallets used up to the present. The modern hammers have a wood core covered with one or two layers of compressed wool felt, whose stiffness increases from heavy bass hammers to light treble hammers to produce a good tone [1]. One of the most important features of the hammer felt is the ability to provide much brighter sound for strong impact than it does for weak impact forces. It means that the felt stiffness increases also with the rate of loading.

First constitutive framework proposed to mathematical model of the hammer felt was made by Ghosh [2], who considered the force-compression characteristic of the felt obeying the power law form

$$F = Ku^p, \tag{1}$$

where  $F$  is the acting force,  $u$  is felt compression, and constant  $K$  has units of  $N/m^p$ . Experimental static testing of different hammers by Hall and Askenfelt [3] demonstrate that for hammers taken from pianos the values of  $p$  ranging from 2.2 to 3.5 give a good approximation of dependence (1).

According to Hertz's Law the force acting on two connected locally Hookean bodies gives  $p = 1.5$ . The values of  $p$  different from 1.5 indicate the non-Hooke or the nonlocal felt properties. Just like these properties of the felt were confirmed experimentally by Yanagisawa, Nakamura and Aiko [4], and by Yanagisawa and Nakamura [5], [6]. Their dynamic experiments demonstrate very important properties of the felt: the nonlinear force-compression characteristic, strong dependence of the slope of the loading curve on the rate of loading, and

significant influence of hysteresis, i.e., the loading and unloading of the felt are not alike. These phenomena require that the felt made of wool is a microstructural material possessing history-dependent properties. The dynamic behavior of such solid matter is highly sensitive to characteristic frequency and rate of loading, and for this reason the concept of an almost unique force-compression curve for a given material does not exist.

Following Rabotnov [7], in [8] the new hysteretic model of the felt is proposed by replacing of the constant parameter  $K$  in expression (1) by a time-dependent operator  $F_0[1 - R(t)*]$ , where  $*$  denotes the convolution, and the relaxation function given by

$$R(t) = (\varepsilon/\tau_0) \exp(-t/\tau_0). \quad (2)$$

Thus, instead of the simple relation (1) we have the four-parameter hereditary model of the felt in the form [8],

$$F(u(t)) = F_0 \left[ u^p(t) - \frac{\varepsilon}{\tau_0} \int_0^t u^p(\xi) \exp\left(\frac{\xi - t}{\tau_0}\right) d\xi \right]. \quad (3)$$

Here the instantaneous stiffness  $F_0$  and compliance nonlinearity exponent  $p$  are the elastic parameters of the felt, and hysteresis amplitude  $\varepsilon$  and relaxation time  $\tau_0$  are the hereditary parameters. According to this model, a real piano hammer felt possesses history-dependent properties, or in other words, is a material with memory.

In [8], it was shown that this constitutive model of felt clarifies the dynamic features of piano hammers fairly well, and is consistent also with experiments [4]–[6].

## 2 Experimental results

For the experimental study of the dynamic felt features the piano hammer testing device described in [9] was used. This device permits to measure the force-time and compression-time dependencies, and investigate the force-compression characteristics of the felt under the rates of loading ranging from 0.3 m/s to 1.5 m/s. The precision of the felt compression determination is equal to  $\pm 10 \mu\text{m}$ ; the acting force up to 60 N is measured with the accuracy of 6%; the time sampling rate is equal to  $7 \mu\text{s}$  (the precision of the signal processor time scale is  $\pm 0.1 \mu\text{s}$ ).

In Fig. 1, the experimental results of the felt examining at the rate of loading 1.32 m/s, 0.99 m/s, and 0.72 m/s are displayed. Of course, these velocities do not cover the real range, which is up to 5 m/s in grand pianos. But, as the hammer strikes the flexible string in grand piano, the value of the acting force exceeds 60 N very seldom. In our case, the hammer strikes the rigid immovable object, thus the acting force and felt compression achieve the maximum values at smaller velocity. In Fig. 1, we can see the really hard blow (felt compression up to 0.9 mm) for the hammer velocity of 1.32 m/s.

The arrows in Fig. 1c indicate the direction of the compression process. The solid lines here represent the numerical simulation of the experiment, and will be interpreted further.

The experimental results presented in Fig. 1 are quite typical for all the hammers measured. The relationships of dynamic force versus felt compression show the significant influence of hysteresis characteristics, so the loading and unloading of the felt (shown by arrows) are not alike. Moreover, the slope of the force-compression characteristics increases with the growth of the hammer velocity, just like the model of the hysteretic hammer predicts. Figure 1c is very similar to Fig. 7b from [5], and both are similar to Fig. 2a from [8], and thus it is evident, that the experiments confirm fairly well the theory.

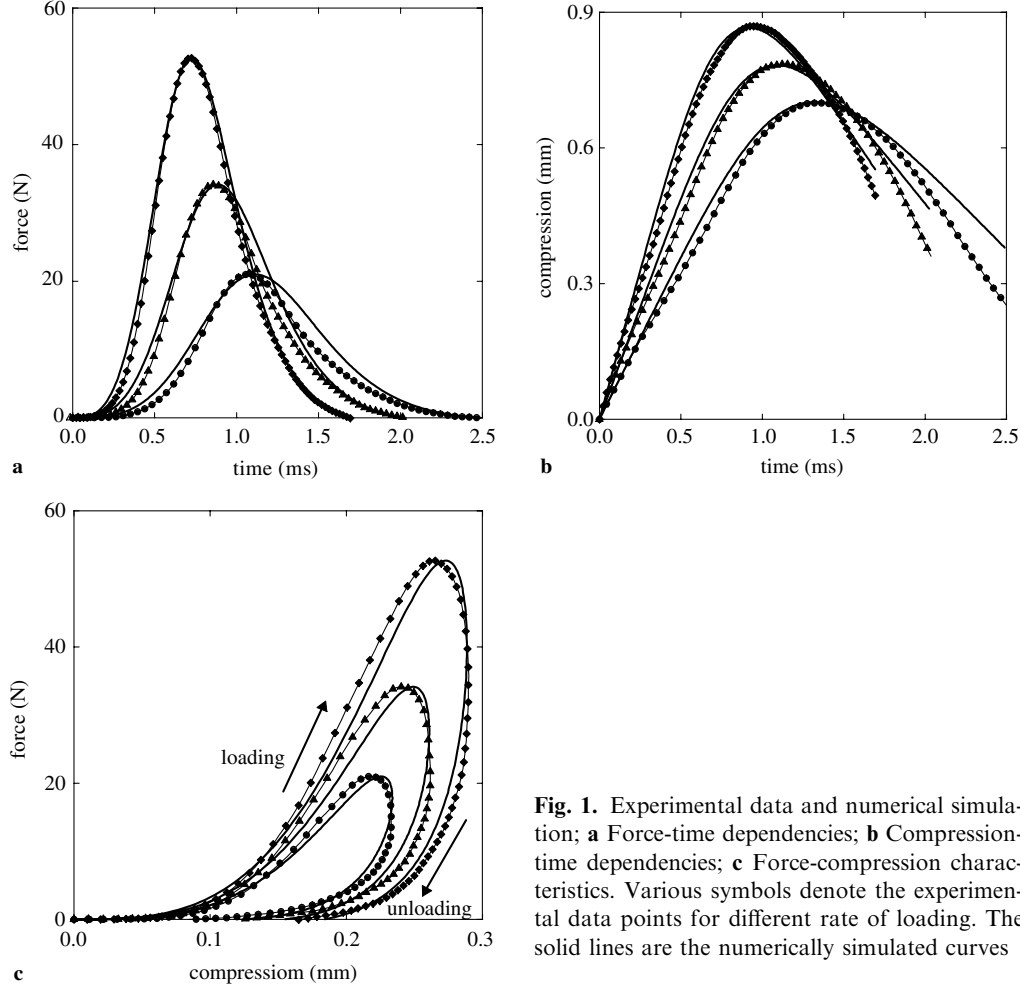


**Fig. 1.** Experimental data and numerical simulation; **a** Force-time dependencies; **b** Compression-time dependencies; **c** Force-compression characteristics. Various symbols denote the experimental data points for different rate of loading. The solid lines are the numerically simulated curves

Figure 1b demonstrates that the initial parts of the compression histories are close to linear function. It indicates that the rate of the felt compression is equal to the initial hammer velocity for a rather long time, and therefore the outer layers of the felt are quite smooth enough. Figure 1 illustrates also a very important dynamic feature of the felt: the maximum of the felt compression follows the maximum of the acting force, and the felt is still deformed after the force is removed. The moment, when the acting force is disappeared we denote here as  $t_0$ . After this moment the felt unloads freely by exponential law. It is following Eq. (3). In case of  $F(t) = 0$  for any  $t \geq t_0$  we have

$$u^p(t) = \frac{\varepsilon}{\tau_0} \int_{t_0}^t u^p(\xi) \exp\left(-\frac{\xi-t}{\tau_0}\right) d\xi, \quad (4)$$

that yields

$$u(t) = u_0 \exp\left[-\frac{(1-\varepsilon)(t-t_0)}{p\tau_0}\right], \quad (5)$$

where  $u_0 = u(t_0)$ .

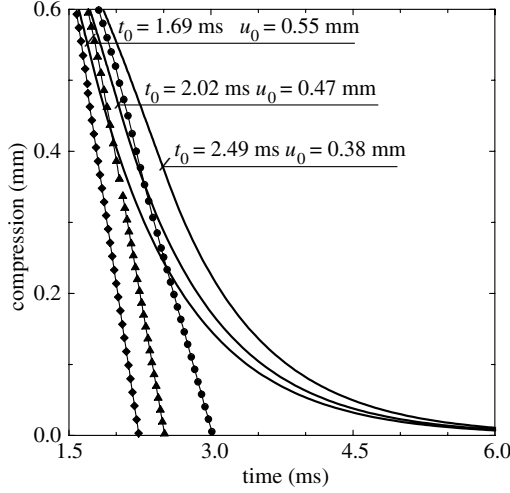


**Fig. 2.** Free decomposition of the felt. The solid lines are the theoretical dependencies. Various symbols denote the experimental data points and show only the hammer translation

Unfortunately, our experimental arrangement does not give the possibility to register the free felt decomposition. We can determine the felt compression as the difference between the initial hammer position just before the strike (the level of the force sensor) and the current position only. After the moment  $t_0$  the hammer loses the contact with the force sensor and moves away. The absolute value of the rate of the felt decomposition at this moment is less than the absolute value of the hammer velocity (the velocity of decomposition may be determined using Eq. (5)), and thus the hammer does not act on the force sensor. The real values of the hammer velocity and the rate of free decomposition of the felt will be discussed also below.

During the experiments dozens of piano hammers produced by various firms were tested, and it was found [10] that the felt of all hammers possesses the same hysteretic properties, or just as well, the felt made of wool is of a material with memory. It seems that using such a felt material for the hammer manufacturing during more than a hundred years is a really indispensable substance.

### 3 Numerical simulation of the experiments

The felt parameters may be obtained by numerical simulation of the dynamic experiments. This procedure was presented in [8], [9] and it is based on the mathematical model of the experiment. The impact of the hammer can be described by the equation of motion

$$m \frac{d^2 u}{dt^2} - F(u) = 0, \quad (6)$$

with the initial conditions

$$u(0) = 0, \quad \frac{du}{dt}(0) = V_0. \quad (7)$$

Here  $m$  and  $V_0$  are the hammer mass and velocity, respectively, and  $F(u)$  is defined by Eq. (3).

The initially unknown values of the elastic and hereditary felt parameters were obtained by means of numerical simulation of the model. The force-compression characteristics  $F(u)$  was numerically calculated from Eq. (6) by assuming some initial values of parameters. The model

was run repeatedly, each time with different parameter values, until the prediction from the model gave a good agreement with the experimental data.

At the same time we must remember that each force-compression curve is composed by using two experimentally obtained curves – the force-time and compression-time curves. These curves are presented in Fig. 1a and b, marked differently for each velocity. We must provide the numerical simulation of Eq. (6) so that the good agreement with the experiment for both of the curves is obtained simultaneously. It means that not only the similar forms of the theoretical and experimental curves (force and compression histories together) should be obtained, but also the duration of the theoretical contact time must be the same (or close enough to the experimental value). The real difference between the contact times achieved by simulation does not exceeded  $\pm 0.01$  ms.

The simulated curves presented in Fig. 1 by solid lines were calculated by using one certain combination of felt parameters. Only the value of hammer velocity was varied. The values of parameters denoted here as set Ia are displayed in Table 1 in the first column. It is interesting, that the value of the relaxation time  $\tau_0$  obtained is approximately a thousand times less than the contact time of interaction, which is equal to 1.7 ms for the hammer speed 1.32 m/s and 2.5 ms for the hammer speed 0.72 m/s.

Now, having the exact values of the felt parameters we can estimate the rate of the felt decompression after the moment  $t_0$ , when the acting force is vanished. In Fig. 2, there is presented the resumption of compression histories shown in Fig. 1b. The solid lines here represent the free decompression curves calculated according to Eq. (5).

The initial time  $t_0$ , and initial value of the felt compression  $u_0$  are also displayed for each curve on the level, where the free decompression starts. The beginning rate of the free felt unloading determined by the differentiation of Eq. (5) is equal to  $-0.56$  m/s,  $-0.47$  m/s, and  $-0.38$  m/s for the initial hammer velocity 1.32 m/s, 0.99 m/s, and 0.72 m/s, respectively. At this moment the current hammer velocity is equal to  $-0.89$  m/s,  $-0.76$  m/s, and  $-0.48$  m/s for corresponding curves, and remains almost constant. Thus the felt loses the contact with the force sensor, and unloads freely. The residual felt compression achieves the level of the measurement accuracy  $10 \mu\text{m}$  in 6 ms approximately.

The presented analytical four-parameter model (model I) defined by Eq. (3) really describes the dynamic behavior of such a microstructural material as hammer felt, and it is suitable for numerical simulation of the experimental data. It is also evident that in according to this model some certain set of the felt parameters and a definite rate of loading appoints to one and only unique force-compression curve. It seems that each force-compression curve results in a unique combination of felt parameters and vice versa.

However not all is so simple. In spite of this almost evident supposition, the numerical simulation of the felt impact demonstrates that very similar (by eye) force-compression curves can be obtained using the different sets of felt parameters. For example, it was found that the

**Table 1.** Felt parameters

Model I		Model II
Set Ia	Set Ib	Set II
$F_0 = 8800 \text{ N/mm}^p$	$F_0 = 3520 \text{ N/mm}^p$	$Q_0 = 70.4 \text{ N/mm}^p$
$p = 3.95$	$p = 3.95$	$p = 3.95$
$\tau_0 = 2 \mu\text{s}$	$\tau_0 = 5 \mu\text{s}$	$\alpha = 250 \mu\text{s}$
$\varepsilon = 0.992$	$\varepsilon = 0.98$	

experimental results presented in Fig. 1 can be simulated also by using another felt parameters denoted as set Ib, and displayed in Table 1 in the second column. A close and subtle analysis of this phenomenon results in a new and quite another hysteretic model of the felt.

#### 4 Three-parameter felt model

Eliminating the integral term, Eq. (6) with the function (3) may be written also in the form

$$m \frac{d^2 u}{dt^2} + m \tau_0 \frac{d^3 u}{dt^3} - F_0 \left[ (1 - \varepsilon) u^p + \tau_0 \frac{d(u^p)}{dt} \right] = 0. \quad (8)$$

The analysis of this equation shows that the second term is much smaller than the first one, and also the other terms. This fact corresponds to the non equality  $F(t) \gg \tau_0 dF/dt$ , which is valid for all values of  $\tau_0$  that are rather small in comparison with  $t_0$ , and for any reasonable value of the felt rate loading – up to 10 m/s. Therefore, the second term may be ignored, and introducing the new parameters

$$Q_0 = F_0(1 - \varepsilon), \quad (9)$$

and

$$\alpha = \tau_0/(1 - \varepsilon), \quad (10)$$

instead of Eq. (8) we have

$$m \frac{d^2 u}{dt^2} - Q_0 \left[ u^p + \alpha \frac{d(u^p)}{dt} \right] = 0. \quad (11)$$

Thus, according to Eq. (6) we can determine the new model of the felt in the form

$$Q(u(t)) = Q_0 \left[ u^p + \alpha \frac{d(u^p)}{dt} \right], \quad (12)$$

where  $Q(u)$  is the force exerted by the hammer,  $Q_0$  is the static hammer stiffness, and  $\alpha$  is the retarded time parameter. Similar to model I, this model of the felt can also be simply proposed by replacing of the constant parameter  $K$  in expression (1) by a time-dependent operator  $Q_0[1 + \alpha D]$ , where  $D$  denotes time differentiation.

Such hysteretic model II is very similar to nonlinear Voigt model and permits a description of the felt compression that is consistent also with experiments. For example, the simulation of the experimental data shown in Fig. 1 may be provided for the same hammer velocities by using the felt parameters denoted as set II, and displayed in Table 1 in the third column. It is more important, however, that these simulated curves are not only exactly alike (by eye) as presented above by solid lines in Fig. 1, but they are also specified by this set of felt parameters uniquely indeed. Now it is clear the cause of existence of different sets of parameters (set Ia and set Ib) similar describing in frame of the first model the dynamic felt behavior. It is evident that both sets of these parameters are equally related by Eq. (9) and Eq. (10) with set II.

#### 5 Two models comparison

Both of the models describe the dynamic felt behavior in a similar way. For example, in Fig. 3 there are presented three hysteretic force-compression characteristics calculated for the three

sets of parameters displayed in Table 1. The hammer mass for this case is equal to 12 g, and the initial hammer velocity is 2.5 m/s.

Really we can see here only one hysteretic force-compression characteristic curve presented by a mixture of various symbols. It is evident that for this hammer velocity these three different sets of felt parameters result in the same (or very alike) force-compression characteristics.

In case of very slow compression, the loading and unloading of the felt are near the limit curve denoted here as *slow loading*, and that is exactly the same curve for both models and for each set of the hammer parameters. Equation of this limit curve may be obtained using Eq. (8) written in the form

$$F + \tau_0 \frac{dF}{dt} - F_0 \left[ (1 - \varepsilon)u^p + \tau_0 p u^{p-1} \frac{du}{dt} \right] = 0. \quad (13)$$

Thus, for the stationary loading the second and last terms vanish, and we have

$$F(u) = F_0(1 - \varepsilon)u^p, \quad (14)$$

or taking into account equality (9) for the model II we have just the same curve

$$Q(u) = Q_0 u^p. \quad (15)$$

For very fast loading these two models are quite different, however. The instantaneous force-compression curve for the first model is given by equation

$$F(u) = F_0 u^p. \quad (16)$$

Such two limit curves denoted here as *fast loading* corresponding to set Ia and set Ib are presented also in Fig. 3, and marked Ia and Ib, respectively. With the increasing of the rate of loading the position of these curves do not make changes, but only their amplitude is increased.

On the contrary, the limit curve for the fast loading in the frame of the model II does not exist at all, because the acting force  $Q(u)$  is proportional to the rate of loading and its value is unlimited. It can be derived using constitutive equation (12). For the fast loading the second term is greater than the first one, and also the rate of compression  $du/dt$  is equal to the hammer velocity  $V_0$ . Thus we have

$$Q(u) = p\alpha V_0 Q_0 u^{p-1}. \quad (17)$$

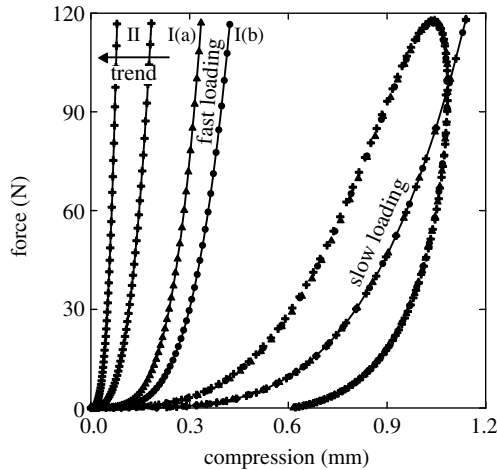


**Fig. 3.** Force-compression characteristics calculated using different sets of felt parameters. Circles, triangles, and crosses correspond to set Ia, set Ib, and set II, respectively

For very fast compression, the loading and unloading of the felt occur near the curve which position tends to the force axis. Two such force-compression curves marked II calculated for the hammer velocities 250 m/s and 3000 m/s are also displayed in Fig. 3.

Two models similarity can be demonstrated also by the example of the free felt decompression. It is easy to show, that in frame of the model-II free decompression of the felt obeys to the same exponential law Eq. (5), which describes the unloading of the felt in according to the four-parameter model. When the acting force is disappeared ( $Q(u) = 0$ ), using Eq. (12) we can find

$$u(t) = u_0 \exp\left[-\frac{(t - t_0)}{p}\right], \quad (18)$$

and it is exactly the same dependence (5), taking into account equality (10).

As far as the models application concerned, a three-parameter model is not only the simpler one, but also it is significantly more suitable for practical numerical calculations. It follows from the large value difference of the time-dimensional parameters  $\tau_0$  and  $\alpha$ . These values were determined using the experimental data, and it was found that the value of parameter  $\alpha$  is at least hundred times greater than the value of parameter  $\tau_0$  (see Table 1). For this reason the numerical simulation of the dynamic felt loading describing by the three-parameter model we may provide applying the much larger time sampling rate than in case of using the four-parameter model.

Using only the general consideration it is very difficult to choose which model is more physical and reasonable by nature. To decide this problem and to prefer the correct model new additional experiments with a very fast felt loading must be provided.

## 6 Conclusions

It has been shown that the dynamic behavior of the piano hammer felt compression, which is essentially hysteretic, can be described by different mathematical models. Two models demonstrated here make predictions in good agreement with experimental data for various types of piano hammers and for the reasonable values of hammer velocities.

Both of the models are quite equivalent for the slow loading of the felt and describe the free felt decompression equally. Quite the contrary, for the fast loading these models give the different description of the felt behavior. However, this difference can be observed only at very high rates of the felt loading, which never occur in case of real playing of piano. Unfortunately, our experimental arrangement can not provide such a fast loading of the felt to decide which model describes the felt behavior more correctly.

Nevertheless, we can use both of the models to describe the dynamic felt compression at the rate of loading up to 10 m/s. Perhaps experiments with new refined and more precise facility can solve the problem of the felt behavior under very fast loading.

## Acknowledgement

This research has been supported by the Estonian Science Foundation under Grant No. 5566.

## References

- [1] Conklin, H. A. Jr.: Design and tone in the mechanoacoustic piano. Part I. Piano hammers and tonal effects. *J. Acoust. Soc. Amer.* **99**, 3286–3296 (1996).
- [2] Ghosh, M.: An experimental study of the duration of contact of an elastic hammer striking a damped pianoforte string. *Indian J. Phys.* **7**, 365–382 (1932).
- [3] Hall, D. E., Askenfelt, A.: Piano string excitation. V. Spectra for real hammers and strings. *J. Acoust. Soc. Am.* **83**, 1627–1638 (1988).
- [4] Yanagisawa, T., Nakamura, K., Aiko, H.: Experimental study on force-time curve during the contact between hammer and piano string. *J. Acoust. Soc. Jpn.* **37**, 627–633 (1981).
- [5] Yanagisawa, T., Nakamura, K.: Dynamic compression characteristics of piano hammer. *Trans. Musical Acoust. Technical Group Meeting of Acoust. Soc. Jpn.* **1**, 14–18 (1982).
- [6] Yanagisawa, T., Nakamura, K.: Dynamic compression characteristics of piano hammer felt. *J. Acoust. Soc. Jpn.* **40**, 725–729 (1984).
- [7] Rabotnov, Yu. N.: *Elements of hereditary solid mechanics*, chap. 17. Moscow: MIR Publishers 1980.
- [8] Stulov, A.: Hysteretic model of the grand piano hammer felt. *J. Acoust. Soc. Am.* **97**, 2577–2585 (1995).
- [9] Stulov, A., Mägi, A.: Piano hammer testing device. *Proc. Estonian Acad. Sci. Engng* **6**, 259–267 (2000).
- [10] Stulov, A., Mägi, A.: Piano hammer: Theory and experiment. In: *Musical sounds from past millennia 1* (Bonsi, D., Gonzalez, D., Stanzial, D., eds.), pp. 215–220. *Int. Symp. on Musical Acoustics*, Perugia, Italia, 2001. Venezia 2001.

**Author's address:** A. Stulov, Centre for Nonlinear Studies, Institute of Cybernetics at Tallinn University of Technology, Akadeemia tee 21, 12618 Tallinn, Estonia (E-mail: stulov@ioc.ee)